



Cite this: RSC Adv., 2021, 11, 23

Received 19th November 2020
Accepted 11th December 2020

DOI: 10.1039/d0ra09819a

rsc.li/rsc-advances

Melodinines Y₁–Y₄, four monoterpene indole alkaloids from *Melodinus henryi*†

Fa-Lei Zhang, Juan He, Tao Feng * and Ji-Kai Liu*

Melodinines Y₁–Y₄ (1–4), four undescribed alkaloids were isolated from *Melodinus henryi*. Their structures were elucidated by extensive NMR, mass spectroscopic analyses, theoretical NMR and electronic circular dichroism (ECD) calculations. Compounds 1 and 2 are the first examples of bisindole alkaloids possessing an eburnamine–leuconoxine combination. Compound 3 is a rare 2,3-seco pleiocarpamine type monoterpenoid indole alkaloid. Compound 1 showed cytotoxic activities against six human cancer cell lines with IC₅₀ values of 0.5–15.2 μ M.

Introduction

Monoterpene indole alkaloids (MIAs) are undoubtedly an important class of natural products that have attracted much attention due to their structural diversity and remarkable biological activity.¹⁻⁴ The genus *Melodinus* (Apocynaceae) contains 53 species all over the world, 11 of which are mainly distributed in southern China and some of them have been used to treat conditions such as bellyache, dyspepsia, orchitis, and rheumatic heart disease and as a Chinese folk medicine.⁵ It has been demonstrated that plants of the genus *Melodinus* are rich in MIAs.⁶ So far, more than 280 MIAs have been obtained from these plants.⁶⁻⁹ Of them, over 40 bisindole alkaloids, comprised by two MIA units, have been identified, and most of them have been reported to demonstrate cytotoxicity against several human cancer cell lines *in vitro*.⁶⁻⁹

M. henryi is a cane distributed in China, Thailand, and Burma. The fruits of *M. henryi* is used for treating meningitis and fracture in China.¹⁰ Previous chemical investigations on this plant reported a series of MIAs with new carbon skeletons and significant bioactivities.⁹⁻¹⁷ For instance, melohenine A was isolated as a novel C₂₄ MIA with a rigid eight-ring system,¹⁷ melohenine B was isolated as a ketolactam derivative, regarded as a key intermediate from indole to quinolone,¹⁷ while melodinine V was a vincanol-eburenine bisindole alkaloids showing selective cytotoxic activities against human HT-29 cells.⁹ It induced cell cycle arrest at G1 phase and cellular apoptosis by increasing histone-associated DNA fragmentation in the treated HT-29 cells.⁹ Inspired by the novel structure and remarkable biological activity, we have been engaged in research on the chemical composition of the plant for a long time.^{11,13,16,17} In the

current study, four new MIAs, melodinines **Y₁–Y₄** (**1–4**), have been isolated from the bark of *M. henryi* (Fig. 1). Their structures with absolute configurations were elucidated by means of spectroscopic and computational methods. Melodinines **Y₁** and **Y₂** (**1** and **2**) are two novel bisindole alkaloids representing the first example of an eburnamine–leuconoxine combination. Melodinine **Y₃** (**3**) is a rare 2,3-*seco* pleiocarpamine type MIA. All compounds were evaluated for their cytotoxicity against six human cancer cell lines. Herein, the isolation, structural elucidation, and biological activities of these compounds are reported.

Results and discussion

The molecular formula of compound **1** was established as $C_{39}H_{50}N_4O_2$ by the positive high resolution (HR) ESI mass spectrum, indicating 17 degrees of unsaturation. It's UV absorption bands at 293 and 207 nm suggesting an indole

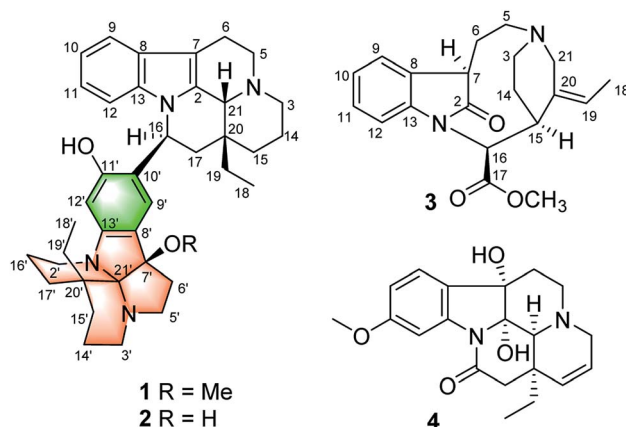


Fig. 1 Compounds 1–4 isolated from *M. henryi*.

Table 1 ^1H and ^{13}C NMR data of **1** and **2** (methanol- d_4 , δ in ppm and J in Hz)

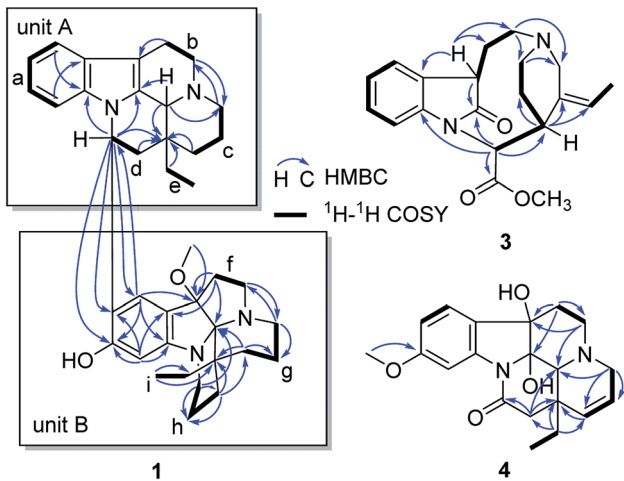
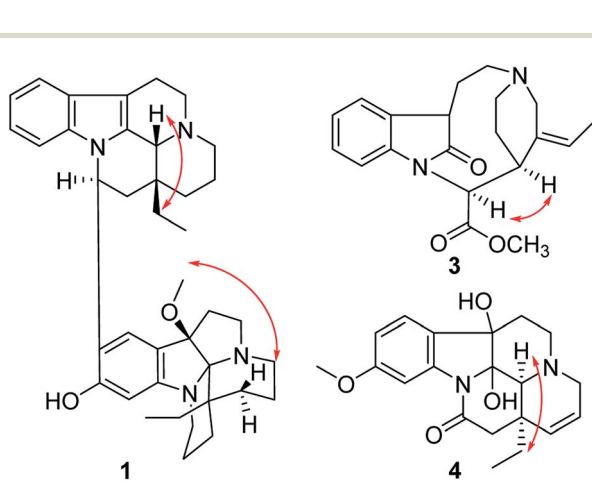
Unit A				Unit B					
No.	1 δ_{H}	1 δ_{C}	2 δ_{H}	2 δ_{C}	No.	1 δ_{H}	1 δ_{C}	2 δ_{H}	2 δ_{C}
2		131.9 s		132.3 s	2'	2.97 m; 3.26 m	58.2 t	3.24 m; 3.63 m	57.7 t
3	2.58 t (10.0); 2.80 m	45.5 t	2.57 m; 2.77 m	45.4 t	3'	2.75 m; 3.45 m	63.6 t	3.27 m	61.7 t
5	3.46 m	52.0 t	3.42 m	51.9 t	5'	2.91 m; 3.33 m	64.5 t	3.02 m; 3.49 m	63.5 t
6	2.82 m; 3.03 m	17.6 t	2.81 m; 3.04 m	17.7 t	6'	2.39 m; 2.48 m	34.0 t	2.30 m; 2.60 m	39.2 t
7		105.2 s		105.1 s	7'		94.3 s		90.4 s
8		129.3 s		129.2 s	8'		117.4 s		118.9 s
9	7.41 d (7.8)	119.2 d	7.42 d (8.0)	118.9 d	9'	6.78 s	124.9 d	6.85 s	123.1 d
10	6.94 t (7.8)	120.7 d	6.97 t (8.0)	120.5 d	10'		122.7 s		124.3 s
11	6.81 t (7.8)	121.9 d	6.90 t (8.0)	122.0 d	11'		158.5 s		157.4 s
12	6.63 d (7.8)	113.1 d	6.79 d (8.0)	112.7 d	12'	6.48 s	98.3 d	6.40 s	98.3 d
13		137.7 s		137.9 s	13'		150.8 s		148.1 s
14	1.46 m; 1.82 m	20.6 t	1.47 m; 1.86 m	20.7 t	14'	1.70 m	26.3 t	1.68 m	31.4 t
15	1.15 m; 1.53 m	24.4 t	1.12 m; 1.53 m	24.5 t	15'	1.91 m; 2.41 m	26.9 t	2.14 m; 2.40 m	29.6 t
16	5.55 dd (11.0, 4.5)	49.9 d	5.57 dd (10.8, 4.6)	48.5 d	16'	1.82 m; 2.30 m	20.0 t	1.84 m; 2.41 m	20.7 t
17	1.67 m; 2.37 m	42.7 t	1.73 m; 2.31 m	43.5 t	17'	1.40 m; 1.61 m	33.2 t	1.61 m; 1.84 m	31.9 t
18	0.93 t (7.2)	7.7 q	0.89 t (7.4)	7.7 q	18'	0.89 t (7.4)	7.1 q	0.93 t (7.5)	7.1 q
19	1.54 m; 2.09 m	29.3 t	1.54 m; 2.14 m	29.4 t	19'	1.34 q (7.4)	34.5 t	1.30 m	35.3 t
20		36.4 s			20'		32.8 s		33.0 s
21	4.38 s	61.2 d	4.33 s	61.1 d	21'		103.7 s		102.1 s
				OMe	2.68 s		53.0 q		

chromophore,⁷ and the IR absorption bands at 3418 cm^{-1} indicated NH and/or OH functionalities. The 1D NMR data revealed that **1** possessed three methyl, 16 methylene, 8 methine, and 12 quaternary carbons (Table 1). Compound **1** was identified preferentially as a bisindole alkaloid with a combination of an eburnamine and a leuconoxine unit, similar to isoeburnamine¹⁰ (unit A) and leuconoxine¹⁸ (unit B), after analyzed all of the NMR data.

The ^1H – ^1H COSY spectrum revealed nine partial structures **a**–**i** as shown in Fig. 2. In the ^1H NMR spectrum, four aromatic protons at δ_{H} 7.41 (1H, d, J = 7.8 Hz), 6.94 (1H, t, J = 7.8 Hz), 6.81 (1H, t, J = 7.8 Hz) and 6.63 (1H, d, J = 7.8 Hz) were assigned to be the unsubstituted indole moiety in unit A, which were

further supported by ^1H – ^1H COSY and the key HMBC correlations of δ_{H} 7.41 (1H, d, J = 7.8 Hz, H-9) with δ_{C} 137.7 (s, C-13) and δ_{H} 6.63 (1H, d, J = 7.8 Hz, H-12) with δ_{C} 129.3 (s, C-8). And the key HMBC correlations of δ_{H} 3.03 (1H, m, H-6) and 2.82 (1H, m, H-6) with δ_{C} 105.2 (s, C-7), δ_{H} 4.38 (1H, s, H-21) with δ_{C} 131.9 (s, C-2), 45.5 (t, C-3), and 36.4 (s, C-20) suggested the connections of partial structures **b** and **c** through N-4 atom, and C-21 with N-4 and the connections of C-21 with C-2 and C-21 with C-20. In addition, the HMBC correlations also revealed the connections of structures **c**–**e** and C-21 with C-20. The above data suggested that unit A possessed an eburnan-type skeleton, similar to isoeburnamine.

In the ^1H NMR spectrum, two aromatic protons at δ_{H} 6.78 (1H, s) and 6.48 (1H, s) were assigned to a disubstituted benzene group in unit B (Fig. 2). In the ^{13}C NMR spectrum, eight signals

Fig. 2 Key HMBC and ^1H – ^1H COSY correlations of **1**, **3**, and **4**.Fig. 3 Key ROESY correlations of **1**, **3**, and **4**.

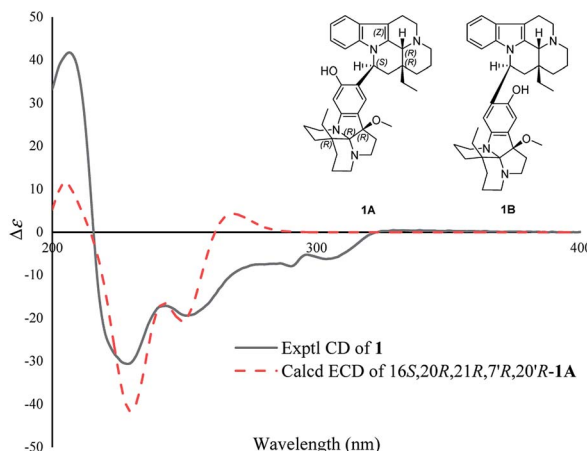


Fig. 4 Comparison of the calculated ECD spectra with the PCM model for **1A** with the experimental spectrum of **1** in methanol.

at δ_{C} 158.5 (s), 150.8 (s), 124.9 (d), 122.7 (s), 117.4 (s), 98.3 (d), 103.7 (s), and 94.3 (s) showed characteristics for an indolenine moiety. A methoxy placed at C-7' was established by the HMBC correlation from δ_{H} 2.68 (3H, $\text{H}_3\text{-OMe}$) to δ_{C} 94.3 (s, C-7'). One sp^3 quaternary carbon at δ_{C} 103.7 (s, C-21') suggested that unit B might have a structure similar to leuconoxine. The HMBC correlations, associated with the ^1H - ^1H COSY data, established unit B as given in Fig. 2. The linkage of between units A and B by the bond C-16/C-10' was established by HMBC correlations of δ_{H} 5.55 (1H, dd, $J = 11.0, 4.5$ Hz, H-16) with δ_{C} 122.7 (s, C-10'), 158.5 (s, C-11'), and 124.9 (d, C-9'), and of δ_{H} 6.78 (1H, s, H-9') with 49.9 (d, C-16). This data also determined the placement for the OH at C-11' unambiguously.

The relative configuration of **1** was elucidated by the ROESY spectrum and the ^1H - ^1H coupling constants. The coupling constant of H-16 (dd, $J = 11.0, 4.5$ Hz) suggested H-16 to be α -oriented by comparison with that of isoeburnamine (dd, $J = 11.5, 4.8$ Hz).¹⁰ The ROESY correlations of H-16/H-15a and H-21/H-19 suggested that H-21 and the ethyl were on the opposite side (Fig. 3).⁷ The ROESY correlation of $\text{H}_3\text{-OMe}/\text{H-15a}'$ suggested that the methoxy and the ethyl were on the same side (β -orientation) in unit B (Fig. 3), the same as that of leuconoxine.

To determine the linkage mode of units A and B, the theoretical NMR calculations and DP4+ probability analyses were employed (see ESI†). The ^{13}C NMR chemical shifts of **1A** and **1B** were calculated at the B3LYP/6-311G(d,p) level with the PCM model in methanol. The calculated results for **1A** ($R^2 = 0.9840$) were a better match with the experimental data than those of **1B** ($R^2 = 0.9649$) (Fig. S3†). Moreover, according to the DP4+ probability analyses, **1A** was assigned with a 100% probability (Table S5†). The messages suggested the **1A** was the correct relative structure for **1**.

The absolute configuration of **1** was determined by ECD calculations. As shown in Fig. 4, the calculated ECD spectrum of (16S,20R,21R,7'R,20'R)-**1A** matched well with the experimental one, suggesting the absolute configuration of **1** to be 16S,20R,21R,7'R,20'R (the ECD curve was simulated in SpecDis V1.71 using a Gaussian function with sigma/gamma value 0.15 eV and a UV shift of -31 nm). Therefore, the structure of compound **1** was identified and named as melodinine Y₁.

Compound **2** was isolated as a white powder, and its molecular formula was established as $\text{C}_{38}\text{H}_{48}\text{N}_4\text{O}_2$ by HRESIMS data, indicating 17 degrees of unsaturation. With the aid of DEPT and HSQC spectra, the 38 carbon resonances as displayed by the ^{13}C NMR spectrum could be ascribed to two CH_3 , sixteen

Table 2 ^1H and ^{13}C NMR data of **3** and **4** (methanol- d_4 , δ in ppm and J in Hz)

No.	3		4	
	δ_{H}	δ_{C}	δ_{H}	δ_{C}
2		184.1 s		93.1 s
3	1.96 m; 2.72 m	46.1 t	2.88 dt (17.0, 2.0); 3.29 d (4.7)	55.7 t
5	1.94 m; 2.21 m	51.7 t	2.59 td (13.0, 3.8); 2.70 dt (11.6, 3.4)	50.3 t
6	2.19 m; 2.55 m	31.9 t	1.60 td (13.0, 3.8); 2.01 dt (11.6, 3.4)	37.5 t
7	3.39 d (5.5)	45.2 d		79.3 s
8		130.1 s		130.9 s
9	7.27 d (7.5)	125.0 d	7.26 d (8.5)	124.0 d
10	7.03 t (7.5)	123.2 d	6.71 dd (8.5, 2.3)	111.3 d
11	7.05 t (7.5)	127.3 d		161.6 s
12	6.68 d (7.5)	114.3 d	7.65 d (2.3)	106.1 d
13		145.8 s		141.2 s
14	1.67 m; 2.25 m	31.0 t	5.77 dd (10.0, 4.7)	125.2 d
15	3.78 d (7.5)	35.2 d	5.47 dt (10.0, 2.0)	135.4 d
16	5.43 br s	63.2 d		170.2 s
17		172.7 s	2.35 d (17.3); 2.91 d (17.3)	45.1 t
18	1.73 dt (7.0, 2.0)	13.9 q	0.96 t (7.3)	9.5 q
19	4.86 m	121.7 d	1.42 dq (14.5, 7.3); 2.28 dq (14.5, 7.3)	34.0 t
20		136.5 s		40.4 s
21	1.60 m; 2.68 m	59.6 t	2.79 s	61.8 d
OMe	3.84 s	53.0 q	3.79 s	56.0 q



CH₂, eight CH, and twelve non-protonated carbons (Table 1). Preliminary analyses of these spectroscopic features implied that **2** had the same carbon skeleton as that of **1**, except that one hydroxy group at C-7' in **2** replaced the methoxy group in **1**, which was supported by the HRESIMS data. Detailed analysis of 2D NMR data suggested that the other parts of **2** were the same to those of **1**. The absolute configuration of **2** was suggested to be 16S,20R,21R,7'R,20'R by comparison with CD curve to that of **1** (see Fig. S32 in the ESI†). Therefore, compound **2** was identified as melodinidine Y₂.

Compound **3** was isolated as a white powder, and the molecular formula of **3** was established as C₂₀H₂₄N₂O₃ by HRESIMS data. The ¹³C NMR and DEPT spectra of **3** displayed 20 carbon resonances ascribed to two CH₃ (including a methoxy), five CH₂, eight CH, and five C (Table 2). The 1D NMR spectra of **3** were very similar to those of the known compound, secopleiocarpamine A,¹⁹ except for the presence of a methylene group rather than a –CN group at C-3 in compound **3**. It was confirmed by the key 2D NMR correlations (Fig. 2). The ROESY correlation of H-15/H-16 suggested that H-15 and H-16 were on the same side (Fig. 3). However, the orientation of H-7 could not be deduced from the ROESY correlations. To determine its final structure, the theoretical NMR calculations and DP4+ probability analyses were employed on two possible structures (*7R,15S,16S*)-**3a** and (*7S,15S,16S*)-**3b**, and the calculations messages suggested that (*7R,15S,16S*)-**3a** was the correct relative structure for **3** (Table S11†). As shown in Fig. 5, the absolute configuration of **3** was suggested to be *7R,15S,16S* by means of ECD calculation. Therefore, compound **3** was identified as melodinidine Y₃.

The molecular formula of **4**, C₂₀H₂₄N₂O₄, was determined by the positive HR-ESI mass spectrum. According to the comparison of the ¹³C NMR spectra with that of Δ^{14} -vincinone,²⁰ the difference between them was two hydroxyl groups replaced the double bonds between C-2 and C-7 in **4**, which was supported by the HRESIMS data. The relative configuration of **4** was determined by the ROESY correlation of H-19/H-21 (Fig. 3), which allowed the configurations of H-21 and ethyl to be assigned as α .

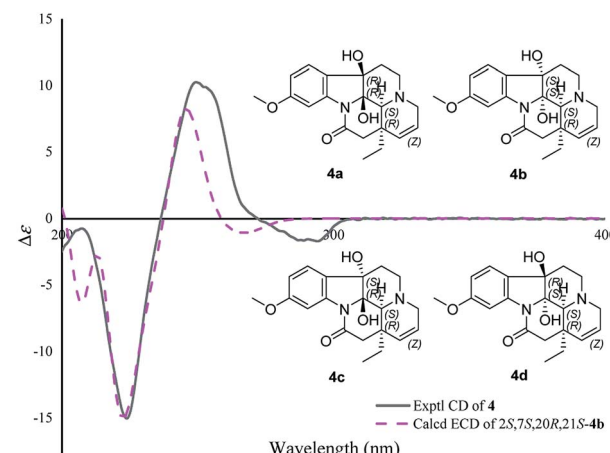


Fig. 6 Comparison of the calculated ECD spectra with the PCM model for **4b** with the experimental spectrum of **4** in methanol.

Table 3 Cytotoxicity of compound **1** (IC₅₀, μ M)

No.	SK-BR-3	SMMC7721	HL-60	PANC-1	A549	MCF-7
1	7.8	7.4	0.5	14.5	14.7	15.2
Cisplatin	22.5	14.1	1.8	19.5	26.5	13.8

However, the relative configuration of the two hydroxyl groups could not be defined by the ROESY data alone. The theoretical NMR calculations and DP4+ probability were employed to determine its final structure. As shown in Fig. S13,† the ¹³C NMR chemical shifts of (*2R,7R,20R,21S*)-**4a**, (*2S,7S,20R,21S*)-**4b**, (*2R,7S,20R,21S*)-**4c** and (*2S,7R,20R,21S*)-**4d** were calculated at the B3LYP/6-311+G(d,p) level with the PCM model in methanol. The calculated results for **4b** ($R^2 = 0.9980$) were a better match with the experimental data than others (Fig. S13†). Moreover, according to the DP4+ probability analyses, **4b** was assigned with a 100% probability (Table S20†). The absolute configuration of **4** was suggested to be *2S,7S,20R,21S* by means of ECD calculation at the B3LYP/6-31+G(d,p)//B3LYP/6-31G(d) level was compared with the experimental ECD curve (Fig. 6). Therefore, compound **4** was identified as melodinidine Y₄.

All compounds were investigated for their cytotoxicity against SK-BR-3, SMMC7721, HL-60, PANC-1, A549, and MCF-7 *in vitro*. As a result, compound **1** showed cytotoxicity toward six cancer cell lines, especially strongly inhibited HL-60 cell with an IC₅₀ value of 0.5 μ M (Table 3). The other compounds were inactive at the concentration of 40 μ M. From the results of compounds **1** and **2**, it can be inferred that the methoxy group at position 7' is the necessary for cytotoxicity.

Conclusions

In summary, four new MIAs including two bisindole alkaloids with an unusual eburnamine–leuconoxine combination, and a rare 2,3-seco pleiocarpamine type alkaloid were isolated from the bark of *Melodinus henryi*. Their structures with absolute

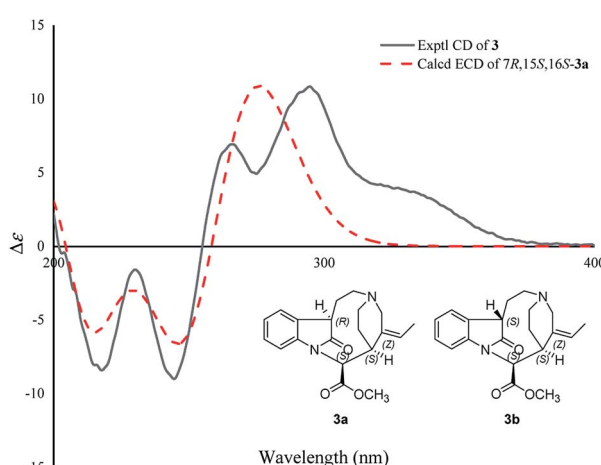


Fig. 5 Comparison of the calculated ECD spectra with the PCM model for **3a** with the experimental spectrum of **3** in methanol.



configurations were established. Compound **1** showed cytotoxicity toward six cancer cell lines. The new modification of the isolated compounds expand the chemical diversity of the MIAs family. Furthermore, cytotoxicity assays have demonstrated that compound **1** significantly inhibited HL-60 cancer cell line, presenting us with a great opportunity to discover promising natural agents for new antitumor leadings.

Experimental section

General experimental procedures

Optical rotations were measured with an Autopol IV polarimeter (Rudolph, Hackettstown, USA). UV spectra were obtained using a Double Beam Spectrophotometer UH5300 (Hitachi High-Technologies, Tokyo, Japan). IR spectra were obtained by a Shimadzu IRTtracer-100 spectrometer using KBr pellets. CD spectra were recorded with an Applied Photophysics Chirascan-Plus CD Spectrometer (Chirascan, New Haven, USA). ¹D and ²D NMR spectra were run on a Bruker Avance III 600 MHz spectrometer or on a Bruker DRX-500 spectrometer with TMS as an internal standard. Chemical shifts (δ) were expressed in ppm with reference to solvent signals. High resolution electrospray ionization mass spectra (HRESIMS) were recorded on an Agilent 6200 Q-TOF MS system or a LC-MS system consisting of a Q ExactiveTM Orbitrap mass spectrometer with a HESI ion source (ThermoFisher Scientific, Bremen, Germany). HREIMS was recorded on a Waters Auto Premier P776 spectrometer or on an API QSTAR Pulsar I spectrometer. Column chromatography (CC) was performed on silica gel (200–300 mesh, Qingdao Marine Chemical Ltd., Qingdao, People's Republic of China), RP-18 gel (20–45 μ m, Fuji Silysia Chemical Ltd., Japan), and Sephadex LH-20 (Pharmacia Fine Chemical Co., Ltd., Sweden). Medium Pressure Liquid Chromatography (MPLC) was performed on a Büchi Sepacore System equipping with pump manager C-615, pump modules C-605 and fraction collector C-660 (Büchi Labortechnik AG, Flawil, Switzerland). Preparative High Performance Liquid Chromatography (prep-HPLC) was performed on an Agilent 1260 liquid chromatography system equipped with Zorbax SB-C18 columns (5 μ m, 9.4 mm \times 150 mm or 21.2 mm \times 150 mm) and a DAD detector. Fractions were monitored by TLC (GF 254, Qingdao Haiyang Chemical Co., Ltd. Qingdao), and spots were visualized by Dragendorff's reagent.

Plant material

The bark of *M. henryi* was collected from Mengla County, Yunnan province, P. R. China on August 12th, 2017. The plant was identified by Mr Yu Chen of Kunming Institute of Botany, Chinese Academy of Sciences. A voucher specimen (No. YChen20170812.Mhb) has been deposited at School of Pharmaceutical Sciences, Chinese Academy of Sciences.

Extraction and isolation

The powdered bark of *M. henryi* (10.0 kg) were extracted three times with 90% EtOH. The combined extracts were concentrated under reduced pressure, and adjusted to pH = 2–3 with

5% HCl. The acidic mixture was defatted with ethyl acetate (EtOAc) and then basified to pH = 9–10 with 10% ammonia solution. The aqueous phase was subsequently extracted with EtOAc to give an alkaloidal extract (201.3 g). The crude alkaloids were then subjected to a silicagel column (200–300 mesh) using CHCl₃–MeOH gradient (1 : 0–0 : 1) to obtain five fractions (A–E). Fraction C (5.1 g) was separated by silica gel CC (petroleum ether–Me₂CO, 20 : 1–0 : 1) to afford subfractions C-1–C-3. Subfraction C-2 was purified on a preparative C18 HPLC column with a gradient of MeCN–H₂O (60 : 40) to yield **1** (3.0 mg, retention time (t_R) = 16.5 min) and **2** (1.5 mg, t_R = 22.1 min). Subfraction C-3 was purified on a preparative C18 HPLC column with a gradient of MeCN–H₂O (50 : 50) to yield **3** (2.0 mg, t_R = 14.5 min) and **4** (2.2 mg, t_R = 26.3 min).

Melodinine Y₁ (**1**). White powder; $[\alpha]_D^{25.5} -237.2$ (c 0.20, CH₃OH); UV (CH₃OH) λ_{max} (log ϵ) 293 (3.60), 207 (4.49) nm; IR (KBr) ν_{max} 3418, 2926, 1624, 1456, 1384, 1319, 1180 cm⁻¹; ¹H NMR (500 MHz) and ¹³C NMR (100 MHz) data (CD₃OD), see Table 1; positive ion HRESIMS m/z 607.4013 [M + H]⁺ (calcd for C₃₉H₅₁N₄O₂, 607.4012).

Melodinine Y₂ (**2**). White powder; $[\alpha]_D^{25.5} -62.6$ (c 0.20, CH₃OH); UV (CH₃OH) λ_{max} (log ϵ) 374 (2.69), 294 (3.68), 207 (4.49) nm; IR (KBr) ν_{max} 3422, 3246, 2937, 1626, 1457, 1308, 1136, 745 cm⁻¹; ¹H NMR (500 MHz) and ¹³C NMR (100 MHz) data (CD₃OD), see Table 1; positive ion HRESIMS m/z 593.3879 [M + H]⁺ (calcd for C₃₈H₄₉N₄O₂, 593.3855).

Melodinine Y₃ (**3**). White powder; $[\alpha]_D^{25.8} +230.9$ (c 0.04, CH₃OH); UV (CH₃OH) λ_{max} (log ϵ) 255 (2.99), 210 (3.49) nm; IR (KBr) ν_{max} 3460, 2090, 1637, 1016, 615 cm⁻¹; ¹H NMR (600 MHz) and ¹³C NMR (150 MHz) data (CD₃OD), see Table 2; positive ion HRESIMS m/z 341.18587 [M + H]⁺ (calcd for C₂₀H₂₅N₂O₃⁺, 341.18597).

Melodinine Y₄ (**4**). White powder; $[\alpha]_D^{23.9} +73.3$ (c 0.01, CH₃OH); UV (CH₃OH) λ_{max} (log ϵ) 290 (3.55), 245 (3.79), 220 (4.01), 210 (3.93) nm; IR (KBr) ν_{max} 3350, 2945, 2833, 1666, 1454, 1417, 1114, 1031, 667 cm⁻¹; ¹H NMR (600 MHz) and ¹³C NMR (150 MHz) data (CD₃OD), see Table 2; positive ion HRESIMS m/z 357.18048 [M + H]⁺ (calcd for C₂₀H₂₅N₂O₄⁺, 357.18088).

Cytotoxicity assay

Six human cancer cell lines, human myeloid leukemia HL-60, hepatocellular carcinoma SMMC-7721, lung cancer A-549, breast cancer SK-BR-3, breast cancer MCF-7, and pancreatic cancer PANC-1 cells, were used in the cytotoxic assay. All the cells were cultured in RPMI-1640 or DMEM medium (Hyclone, USA), supplemented with 10% fetal bovine serum (Hyclone, USA) in 5% CO₂ at 37 °C. The assays were performed according to the MTT (3-(4,5-dimethylthiazol-2-yl)-2,5-diphenyl tetrazolium bromide) method in 96-well microplates.²¹ Briefly, 100 μ L of adherent cells was seeded into each well of 96-well cell culture plates and allowed to adhere for 12 h before drug addition, while suspended cells were seeded just before drug addition with an initial density of 1×10^5 cells per mL. Each tumor cell line was exposed to the test compound at concentrations of 0.064, 0.32, 1.6, 8, and 40 μ M in triplicates for 48 h, with cisplatin (Sigma, USA) as a positive control. After each



compound treatment, cell viability was detected and a cell growth curve was graphed. IC₅₀ values were calculated by Reed and Muench's method.²²

Computation methods

¹³C NMR calculation. Conformation search based on molecular mechanics with MMFF force fields were performed for compounds to get stable conformers with populations higher than 1%.^{23,24} Gauge-independent atomic orbital (GIAO) calculations of ¹³C NMR of conformers were accomplished by DFT at the mPW1PW91/6-311+G(d,p) level with PCM model in methanol based on predominant B3LYP/6-31G(d) optimized geometries were performed in Gaussian 16 software package with g09 default keyword.²⁵ The calculated NMR data of these conformers were averaged according to the Boltzmann distribution theory and their relative Gibbs free energy. The ¹H and ¹³C NMR chemical shifts for TMS were also calculated by the same procedures and used as the reference. After calculation, the experimental and calculated data were evaluated by linear correlation coefficients (R^2) and the improved probability DP4+ method.²⁶

ECD calculation. Conformation search based on molecular mechanics with MMFF force fields were performed for compounds to get stable conformers with populations higher than 1%. All these conformers were further optimized by the density functional theory method at the B3LYP/6-31G(d) or B3LYP/6-311G(2d,p) level by Gaussian 16 program package and the ECD were calculated using density functional theory (TDDFT) at B3LYP/6-31+G(d,p) or B3LYP/6-311G(d) level in methanol with IEFPCM model, respectively. The calculated ECD curves were all generated using SpecDis 1.71 program package and the calculated ECD data of all conformers were Boltzmann averaged by Gibbs free energy.²⁷

Conflicts of interest

There are no conflicts to declare.

Acknowledgements

This work was financially supported by the National Key Research and Development Program of China (2017YFC1704007) and the National Natural Science Foundation of China (21961142008, 81872762). The authors thank the Analytical & Measuring Center of School of Pharmaceutical Sciences, South-Central University for Nationalities.

Notes and references

- 1 J. E. Saxton, *Nat. Prod. Rep.*, 1995, **12**, 385–411.
- 2 T. Beckers and S. Mahboobi, *Drugs Future*, 2003, **28**, 767.
- 3 N. I. Mohd and N. I. Magdy, *Mini-Rev. Med. Chem.*, 2004, **4**, 1077–1104.
- 4 S. E. O'Connor and J. J. Maresh, *Nat. Prod. Rep.*, 2006, **23**, 532–547.
- 5 Y. Tsiang, in *Flora of China*, ed P. T. Li, Science Press, Beijing, 1977, vol. 63, pp. 17–30.
- 6 J. H. Jiang, W. D. Zhang and Y. G. Chen, *Trop. J. Pharm. Res.*, 2015, **14**, 2325–2344.
- 7 T. Feng, Y. Li, Y. Y. Wang, X. H. Cai, Y. P. Liu and X. D. Luo, *J. Nat. Prod.*, 2010, **73**, 1075–1079.
- 8 Y. P. Liu, Y. L. Zhao, T. Feng, G. G. Cheng, B. H. Zhang, Y. Li, X. H. Cai and X. D. Luo, *J. Nat. Prod.*, 2013, **76**, 2322–2329.
- 9 Y. P. Liu, G. G. Yue, J. K. Lee, T. Feng, Y. L. Zhao, Y. Li, C. B. Lau and X. D. Luo, *Bioorg. Med. Chem. Lett.*, 2016, **26**, 4895–4898.
- 10 Y. W. Zhang, R. Yang, Q. Cheng and K. Ofuji, *Helv. Chim. Acta*, 2003, **86**, 415–419.
- 11 Q. Shao, R. Ma, X. Wu, F. L. Zhang, Z. H. Li, T. Feng, J. He and J. K. Liu, *Phytochem. Lett.*, 2020, **35**, 53–57.
- 12 J. Q. Yu, X. W. Sun, Z. W. Wang, L. Fang and X. Wang, *J. Asian Nat. Prod. Res.*, 2019, **21**, 820–825.
- 13 J. He, F. L. Zhang, Z. H. Li, H. X. Yang, Q. Shao, T. Feng and J. K. Liu, *Fitoterapia*, 2019, **138**, 104354.
- 14 L. L. Guo, Y. X. Yuan, H. P. He, S. L. Li, Y. Zhang and X. J. Hao, *Phytochem. Lett.*, 2017, **21**, 179–182.
- 15 H. Zhou, H. P. He, Y. H. Wang and X. J. Hao, *Helv. Chim. Acta*, 2010, **93**, 2030–2032.
- 16 T. Feng, X. H. Cai, Y. P. Liu, Y. Li, Y. Y. Wang and X. D. Luo, *J. Nat. Prod.*, 2010, **73**, 22–26.
- 17 T. Feng, X. H. Cai, Y. Li, Y. Y. Wang, Y. P. Liu, M. J. Xie and X. D. Luo, *Org. Lett.*, 2009, **11**, 4834–4837.
- 18 F. Abe and T. Yamauchi, *Phytochemistry*, 1993, **35**, 169–171.
- 19 A. Ahmed, W. Li, F. F. Chen, J. S. Zhang, Y. Q. Tang, L. Chen, G. H. Tang and S. Yin, *Fitoterapia*, 2018, **128**, 1–6.
- 20 M. Zeches, J. Lounkokobi, B. Richard, M. Plat, L. Le Men-Olivier, T. Sevenet and J. Pusset, *Phytochemistry*, 1984, **23**, 171–174.
- 21 T. Mosmann, *J. Immunol. Methods*, 1983, **65**, 55–63.
- 22 L. J. Reed and H. Muench, *Am. J. Hyg.*, 1938, **27**, 493–497.
- 23 W. J. Hehre, *A guide to molecular mechanics and quantum chemical calculations*, Wavefunction, Inc., Irvine, CA, 2003, pp. 1–812.
- 24 Y. Shao, L. F. Molnar, Y. Jung, J. Kussmann, C. Ochsenfeld, S. T. Brown, A. T. B. Gilbert, L. V. Slipchenko, S. V. Levchenko, D. P. O'Neill, R. A. DiStasio Jr, R. C. Lochan, T. Wang, G. J. O. Beran, N. A. Besley, J. M. Herbert, C. Yeh Lin, T. Van Voorhis, S. Hung Chien, A. Sodt, R. P. Steele, V. A. Rassolov, P. E. Maslen, P. P. Korambath, R. D. Adamson, B. Austin, J. Baker, E. F. C. Byrd, H. Dachsel, R. J. Doerksen, A. Dreuw, B. D. Dunietz, A. D. Dutoi, T. R. Furlani, S. R. Gwaltney, A. Heyden, S. Hirata, C.-P. Hsu, G. Kedziora, R. Z. Khaliulin, P. Klunzinger, A. M. Lee, M. S. Lee, W. Liang, I. Lotan, N. Nair, B. Peters, E. I. Proynov, P. A. Pieniazek, Y. Min Rhee, J. Ritchie, E. Rosta, C. David Sherrill, A. C. Simmonett, J. E. Subotnik, H. Lee Woodcock Iii, W. Zhang, A. T. Bell, A. K. Chakraborty, D. M. Chipman, F. J. Keil, A. Warshel, W. J. Hehre, H. F. Schaefer Iii, J. Kong, A. I. Krylov, P. M. W. Gill and M. Head-Gordon, *Phys. Chem. Chem. Phys.*, 2006, **8**, 3172–3191.



25 G. W. T. M. J. Frisch, H. B. Schlegel, G. E. Scuseria, M. A. Robb, J. R. Cheeseman, G. Scalmani, V. Barone, G. A. Petersson, H. Nakatsuji, X. Li, M. Caricato, A. Marenich, J. Bloino, B. G. Janesko, R. Gomperts, B. Mennucci, H. P. Hratchian, J. V. Ortiz, A. F. Izmaylov, J. L. Sonnenberg, D. Williams-Young, F. Ding, F. Lipparini, F. Egidi, J. Goings, B. Peng, A. Petrone, T. Henderson, D. Ranasinghe, V. G. Zakrzewski, J. Gao, N. Rega, G. Zheng, W. Liang, M. Hada, M. Ehara, K. Toyota, R. Fukuda, J. Hasegawa, M. Ishida, T. Nakajima, Y. Honda, O. Kitao, H. Nakai, T. Vreven, K. Throssell, J. A. Montgomery Jr, J. E. Peralta, F. Ogliaro, M. Bearpark, J. J. Heyd, E. Brothers, K. N. Kudin, V. N. Staroverov, T. Keith, R. Kobayashi, J. Normand, K. Raghavachari, A. Rendell, J. C. Burant, S. S. Iyengar, J. Tomasi, M. Cossi, J. M. Millam, M. Klene, C. Adamo, R. Cammi, J. W. Ochterski, R. L. Martin, K. Morokuma, O. Farkas, J. B. Foresman, and D. J. Fox, *Gaussian 16, Revision B.01*, Gaussian, Inc. Wallingford CT, 2016.

26 N. Grimblat, M. M. Zanardi and A. M. Sarotti, *J. Org. Chem.*, 2015, **80**, 12526–12534.

27 T. Bruhn, A. Schaumlöffel, Y. Hemberger and G. Bringmann, *Chirality*, 2013, **25**, 243–249.

